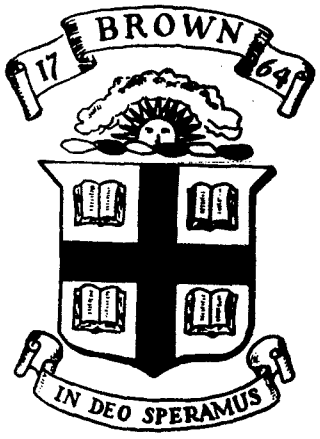

Division of Engineering
BROWN UNIVERSITY
PROVIDENCE, R. I.

IMPACT ON RODS OF NON-LINEAR VISCOPLASTIC MATERIAL NUMERICAL AND APPROXIMATE SOLUTIONS

BY

T.C.T. TING AND P.S. SYMONDS

Department of Defense
Advanced Research Projects Agency
Contract DA-19-020-AMC-0077(R)
ARPA Order No. 71
Supervised by Ballistic Research Laboratories
Aberdeen Proving Ground

Report No. 3

May 1966

I. IMPACT ON RODS OF NON-LINEAR VISCOPLASTIC MATERIAL -- dash

II. NUMERICAL AND APPROXIMATE SOLUTIONS [1]

by

III.
T. C. T. Ting

and

P. S. Symonds. Supervised by Ballistic research laboratories.

III. Ballistic research laboratories.

Technical Report No. 3

May 1966

sponsored by
the Advanced Research Projects Agency
of the Department of Defense and
technically supervised by
Ballistic Research Laboratories,
Aberdeen Proving Ground, through
Contract DA-19-020-AMC-0077(R),
ARPA Order 71.

IMPACT ON RODS OF NON-LINEAR VISCOPLASTIC MATERIAL -- NUMERICAL AND APPROXIMATE SOLUTIONS [1]

T. C. T. Ting [2] and P. S. Symonds [3]

Abstract

A numerical technique is described for the solution of impact on finite rods in which the strain rate is assumed to be a function of stress and strain. Examples are given for the strain rate function taken as a power of the dynamic overstress and the results are compared with available analytic solutions and approximate uniform strain theory.

1. The results presented here were obtained in the course of research sponsored by the Advanced Research Projects Agency of the Department of Defense and technically supervised by Ballistic Research Laboratories, Aberdeen Proving Ground, through Contract DA-19-020-AMC-0077(R), ARPA Order 71.

2. Assistant Professor of Engineering (Research), Brown University; now with University of Illinois at Chicago Circle.

3. Professor of Engineering, Brown University.

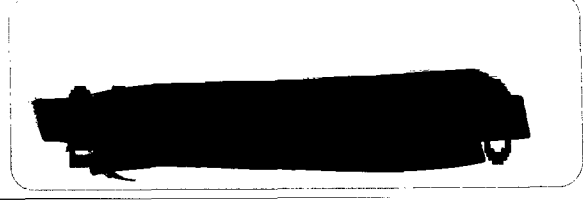

1. Introduction

The behavior of compression impact specimens of material exhibiting rate dependent plastic characteristics is of interest in the design and interpretation of experiments for investigating dynamic plastic properties. Previous studies [1], [2] have presented approaches by way of analytical solutions of the partial differential equations describing the dynamic deformation. Analytical solutions are possible only if the general partial differential equations are linearized, or if approximations are introduced so that the problem is reduced to solving ordinary differential equations. Since the actual behavior of structural metals is strongly non-linear, it is necessary for a realistic treatment to include non-linear relations between stress, strain, and strain rate, as well as irreversibility, in representing the plastic behavior. The present paper describes a scheme of a numerical solution suitable for general viscoplastic laws. The technique is illustrated by computations for two types of viscoplastic law. More extensive calculations and interpretations with experiments will be given in a companion paper.

We consider the problem of impact on a finite rod as shown in Fig. 1. A rigid body of mass G with initial velocity V_o parallel to the axis of the rod strikes at the free end x = 0 of the rod. After contact, the striking mass is assumed to stick to the end of the bar. It is assumed that the input kinetic energy $GV_o^2/2$ is much larger than the maximum elastic energy $\sigma_o^2 AL/2E$ which the rod can absorb. (Here σ_o and E are respectively the static yield stress and the elastic modulus of the rod; A and L are respectively the initial cross sectional area and the length of the rod.) Hence, the elastic strains are assumed negligible in comparison to plastic strains. The material is regarded as rigid-viscoplastic, meaning that no deformation occurs if the dynamic stress is smaller than

the static yield stress and the rate of deformation is governed by a functional relation between strain rate, stress, and strain if the dynamic stress exceeds the static yield stress.

We introduce the following dimensionless notation:

Table 1

$x = \frac{X}{L}$	$t = \frac{\sigma_o T}{\rho D L^2}$	$v = \frac{V}{DL}$	$s = \frac{\sigma}{\sigma_o}$
$k = \frac{G}{\rho A L}$	$\eta = \frac{\sigma_o \varepsilon}{\rho D^2 L^2}$	$v_o = \frac{V_o}{DL}$	$\lambda = \frac{E_1 \rho D^2 L^2}{\sigma_o^2}$

where

X = distance along rod from impact end

T = time

L = length of rod

ρ = mass density of the rod material

G = mass of striking body (assumed rigid)

V = particle velocity at X,T

V_o = initial velocity of striking mass

σ = nominal compressive stress

σ_o = static yield stress in compression (nominal)

ε = nominal compressive strain

D = constant expressing viscoplastic behavior

E_1 = slope of strain hardening curve (tangent modulus in plastic range)

The equations of dynamics and of continuity of velocity are as follows in the dimensionless notation:

$$s_x = - v_t$$
$$\eta_t = - v_x \tag{1}$$

where a subscript denotes partial differentiation. The plastic strain rate behavior will be expressed by means of a function $F(s,\eta)$ such that

$$\eta_t = F(s,\eta) > 0 \quad \text{if } s > g(\eta)$$
$$= 0 \quad \text{if } |s| \leq g(\eta) \tag{2a}$$

where $s = g(\eta)$ is the condition for plastic flow under quasi-static loading, with $g(0) = 1$. $F(s,\eta)$ is assumed to obey the following conditions:

$$F_s > 0$$
$$F_\eta \leq 0 \tag{2b}$$
$$F(g(\eta), \eta) = 0.$$

The form of F which we shall consider in this analysis is

$$\eta_t = (s - 1 - \lambda\eta)^p \quad \text{if } s > 1 + \lambda\eta$$
$$= 0 \quad \text{if } |s| \leq 1 + \lambda\eta \tag{3}$$

where p and λ are constants of the material. The power p corresponds to the non-linearity of the viscoplastic behavior, having values in the neighborhood of 5 for several structural metals (2). The coefficient λ is proportional to the slope of the static stress-strain curve in the plastic range, this being taken as linear for simplicity. For a more general form of F, a material without strain hardening

can be characterized by $F_\eta \equiv 0$.

The initial and boundary conditions of the problem are:

For $0 \leq x \leq 1$:

$$v(x,0) = \eta(x,0) = 0 \tag{4a}$$

$$s(x,0) = 1 \tag{4b}$$

For $0 \leq t$:

$$v(1,t) = 0 \; ; \quad v(0,0) = v_o \tag{4c}$$

$$s(0,t) = - kv_t(0,t) \tag{4d}$$

The boundary condition at $x = 0$ of Eq. (4d) is used as long as $\eta_t(0,t) > 0$. When $\eta_t(0,t) \leq 0$, there is an unloading boundary $\zeta(t)$ (see Fig. 2) along which $\eta_t(\zeta,t) = 0$. Then Eq. (4d) must be replaced by

$$s(\zeta,t) = - (k + \zeta)v_t(\zeta,t). \tag{4e}$$

The numerical solution of Eqs. (1) and (2) subjected to conditions (4) will be discussed in turn in the following sections for materials without strain-hardening ($\lambda = 0$) and with strain-hardening ($\lambda > 0$). The condition (4b) was discussed in [1].

2. No Strain-Hardening

For materials that exhibit no appreciable strain-hardening, the strain rate function F can be assumed independent of η. Hence, instead of Eqs. (2) we write,

$$\begin{aligned} \eta_t &= G(s) > 0 \qquad \text{if } s > 1 \\ &= 0 \qquad\quad \text{if } |s| \leq 1 \end{aligned} \tag{5}$$

where $G_s > 0$ and $G(1) = 0$. Hence, in the region where plastic deformation is occurring, Eqs. (1) and (5) reduce to

$$s_{xx} - G_s(s)s_t = 0 \quad \text{if } s > 1. \tag{6}$$

This is a quasi-linear parabolic equation.

It was shown in [3] that the solution of (6) with the initial and boundary conditions of (4) cannot have an unloading initiated in the interior of a plastic region. The proof depends on the maximum-minimum principles governing equations of the type of Eq. (6) (see [4]).

When Eq. (6) is replaced by a finite difference scheme for numerical calculation, one has to pay attention not only to the convergence and stability of the finite difference equations, but also to the maximum-minimum properties of the equations. Otherwise, physical requirements of the solution may be violated. The maximum-minimum principles for various finite difference equations which approximate Eq. (6) were studied in [5]. The results show that, except for the backward difference method, there is a restriction on the mesh ratio, which depends on $G_s(s)$, in order for the principles to hold. If we denote the mesh ratio $\Delta t/(\Delta x)^2$ by r, the results of [5] show that the weak maximum-minimum principle holds if

$$
\begin{aligned}
&r \le G_s(s)/2 && \text{for the forward method} \\
&r \le G_s(s) && \text{for the Crank-Nicolson method} \\
&\text{any } r && \text{for the backward method.}
\end{aligned}
$$

If $G_s(s)$ is very small for certain s, the mesh ratio must be chosen inconveniently small unless one uses the backward method. For instance, without strain-hardening, Eq. (3) is written as

$$
\begin{aligned}
\eta_t &= (s-1)^p && \text{if } s > 1 \\
&= 0 && \text{if } |s| \le 1.
\end{aligned}
\tag{7}
$$

Hence $G_s(s) = p(s-1)^{p-1}$. For $p > 1$, G_s approaches zero as s approaches one. Therefore, in order to use the same mesh ratio for the whole calculation, we shall use only the backward difference method.

We shall derive the finite difference equations directly from Eqs. (1), and represent the rod for this purpose by a model consisting of discrete mass particles (Fig. 3). Let us divide the rod into n segments (hence $\Delta x = 1/n$) and replace the mass of each segment by a mass particle at the center of the interval. We denote $s_{i,j}$, $\eta_{i,j}$ the stress and strain respectively at the grid point $x = i\Delta x$, $t = j\Delta t$, and we let $v_{i,j}$ denote the velocity at $x = (i - \frac{1}{2})\Delta x$, $t = j\Delta t$. The strain rate will be written as $\dot{\eta}_{i,j}$ instead of using a subscript t. Now, Eqs. (1) and (5), together with the boundary and initial conditions (4c)-(4e) can be written (see Fig. 3) as follows, with $r = \Delta t/(\Delta x)^2$:

Difference equations:

(a) Impulse-momentum, $j = 1,2\ldots$ (8a)

$$i = 0: \quad s_{o,j} = \frac{-n^2 k}{r}\,(v_{o,j} - v_{o,j-1})$$

$$i = 1,2,\ldots n: \quad s_{i,j} - s_{i-1,j} = -\frac{n}{r}\,(v_{i,j} - v_{i,j-1})$$

(b) Viscoplastic behavior, $j = 0,1,2\ldots$ (8b)

$$i = 0,1,2\ldots n: \quad \dot{\eta}_{i,j} = G(s_{i,j}) \text{ if } s_{i,j} > 1$$

$$= 0 \quad \text{if } s_{i,j} \le 1$$

(c) Velocity-strain rate, $j = 1,2\ldots$ (8c)

$$i = 0: \quad v_{1,j} - v_{o,j} = -\frac{1}{2n}\,\dot{\eta}_{o,j}$$

$$i = 1,2\ldots n-1: \quad v_{i+1,j} - v_{i,j} = -\frac{1}{n}\,\dot{\eta}_{i,j}$$

$$i = n: \quad v_{n,j} = \frac{1}{2n}\,\dot{\eta}_{i,j}$$

Initial Conditions ($j = 0$) (9)

$$i = 0: \qquad v_{o,o} = v_o; \quad \dot{\eta}_{o,o} = 2nv_o = G(s_{o,o})$$

$$i = 1,2\ldots n: \qquad v_{i,o} = 0; \quad \dot{\eta}_{i,o} = 0$$

$$s_{i,o} = 1$$

It should be noticed that, with Eqs. (8b), the unloading condition is taken into account and Eq. (4e) is automatically satisfied.

One can eliminate $v_{i,j}$ from Eqs. (8). If this is done one obtains for the general case, with $j = 1,2,\ldots$; $i = 1,2,\ldots n-1$:

$$s_{i+1,j} - 2s_{i,j} + s_{i-1,j} = \frac{1}{r}\left[\dot{\eta}_{i,j} - \dot{\eta}_{i,j-1}\right] \tag{10a}$$

$$= \frac{1}{r}\left[G(s_{i,j}) - G(s_{i,j-1})\right], \tag{10b}$$

making use of Eq. (5), where $G(s_{i,j}) = 0$ if $|s_{i,j}| \leq 1$. Equation (10b) corresponds to the backward finite difference form of Eq. (6). The existence and uniqueness of the solution of $s_{i,j}$ for given $s_{i,j-1}$ of Eqs. (10) were shown in [5].

For given $v_{i,j-1}$, Eqs. (8) can be solved by a method of successive approximations for $v_{i,j}$, $s_{i,j}$ and $\dot{\eta}_{i,j}$. By assuming an approximate value $v_{o,j}^{(o)}$ for $v_{o,j}$, the first equations of Eqs. (8a), (8b) and (8c) give $s_{o,j}^{(o)}$, $\dot{\eta}_{o,j}^{(o)}$, and $v_{1,j}^{(o)}$ respectively. The second equations of Eqs. (8a), (8b) and (8c) then give $s_{1,j}^{(o)}$, $\dot{\eta}_{1,j}^{(o)}$, and $v_{2,j}^{(o)}$. We continue this process until $v_{n,j}^{(o)}$, $s_{n,j}^{(o)}$, and $\dot{\eta}_{n,j}^{(o)}$ are obtained. If the starting value $v_{o,j}^{(o)}$ is the correct one, then the last equation of Eqs. (8c) will be found to be satisfied. In other words, if corresponding to the assumed $v_{o,j}^{(o)}$ we compute $\psi_j^{(o)}$, where

$$\psi_j^{(o)} = v_{n,j}^{(o)} - \frac{1}{2n}\dot{\eta}_{n,j}^{(o)}, \tag{11}$$

and find that $\psi_j^{(o)}$ is zero, we have obtained the solution for time $t = j\Delta t$. Otherwise, we assume another approximation $v_{o,j}^{(1)}$ and repeat the process.

Let δu denote the error, i.e. the difference between a function u and its approximation $u^{(o)}$,

$$\delta u \equiv u - u^{(o)}.$$

Then, from Eqs. (8), one can show (cf. [5]) that

$$\text{if } \delta v_{o,j} > 0,$$

$$\delta\psi \geq \delta v_{n,j} \geq \delta v_{n-1,j} \geq \cdots\cdots\cdots \geq \delta v_{o,j} > 0 \tag{12a}$$

$$\delta s_{n,j} \leq \delta s_{n-1,j} \leq \cdots\cdots\cdots \leq \delta s_{o,j} < b.$$

Similarly, if $\delta v_{o,j} < 0$,

$$\delta\psi \leq \delta v_{n,j} \leq \delta v_{n-1,j} \leq \cdots\cdots\cdots \leq \delta v_{o,j} < 0 \tag{12b}$$

$$\delta s_{n,j} \geq \delta s_{n-1,j} \geq \cdots\cdots\cdots \geq \delta s_{o,j} > 0.$$

In other words, the absolute values of the error in the calculation of $v_{i,j}$ and $s_{i,j}$ increase as i increases. The errors in $v_{i,j}$ are of the same sign. Similarly, the errors in $s_{i,j}$, which have opposite signs to $v_{i,j}$, are of the same sign. With the properties expressed in Eqs. (12) there is no difficulty in the process of successive approximation.

It should be noticed that the successive approximation can be improved by considering other properties, besides Eq. (12), of the solution. For instance, the fact that the unloading boundary must start from x = 0 and terminate at x = 1 implies that

$$\text{if } s_{k,j} \geq 1, \quad s_{i,j} > 1 \text{ for } i > k.$$

Also, it can be shown (see [3]) that for $1 \leq j < N$,

$$v_{i,j} > 0 \quad \text{for} \quad i = 0,1,\ldots..n.$$

At time $t_f = N\Delta t$ all velocities and strain rates are zero, and the deformation stops.

The strains $\eta_{i,j}$ are obtained from

$$\eta_{i,j} = \eta_{i,j-1} + \dot{\eta}_{i,j}\Delta t,$$

which is essentially a backward difference expression for $\dot{\eta}_{i,j}$.

For illustration, the strain rate function of Eq. (7) is taken. In the calculations, p is taken from 1 to 5, $\Delta x = 0.05$ and $\Delta t = 0.025$. To show the accuracy of the numerical calculation for this choice of mesh size, we compare the results for $k = 1$, $v_o = 5$, and $p = 1$ with the exact solution of the differential equation (see [1]), as shown in Fig. 4. Note that the initial condition of the problem for the differential equation is $s(0,0) = \infty$, while that for the finite difference system Eqs. (9) in this example is $s_{o,o} = 201$. Nevertheless, the agreement for the stress distribution is fairly good at $t = 0.1$, which is only four steps from $t = 0$. For $t \geq 0.4$, there is practically no difference between the exact and numerical solutions for both stress and strain in the rod. The time of unloading t_o is 1.665 and the total time of deformation t_f is 2.120 in the exact solution. In the numerical solution, they are 1.680 and 2.128 respectively.

The same mesh size is used in the calculations for p = 1 to 5, with the same impact data $k = 1$, $v_o = 5$. Some of the results are shown in Figs. 5 to 9. Further discussion is deferred to later sections, after the presentation of the solution for strain-hardening.

3. Solutions for Strain-Hardening Materials

For materials that exhibit strain-hardening, the more general strain rate function Eqs. (2) must be used. Although the system of equations cannot now be reduced to a second order parabolic equation in s alone, we shall still use the backward finite difference scheme to approximate the differential equation. This is done so that the solution will exhibit various properties found for non-strain-

hardening materials, when the material has very small but finite strain-hardening.

We use the same model as before, Fig. 3. All of Eqs. (8) are still valid except for Eqs. (8b) which must be replaced by

$$\begin{aligned} \dot{\eta}_{i,j} &= F(s_{i,j}, \eta_{i,j}) \quad \text{if} \quad s_{i,j} > g(\eta_{i,j}) \\ &= 0 \qquad\qquad\quad \text{if} \quad |s_{i,j}| \leq g(\eta_{i,j}) \end{aligned} \tag{8b'}$$

where $\eta_{i,j} = \eta_{i,j-1} + \dot{\eta}_{i,j}\Delta t$. The numerical solution of Eqs. (8a), (8b') and (8c) by successive approximation is essentially the same as that illustrated in the previous section. The only difference is in the calculation of $\dot{\eta}_{i,j}$ by Eqs. (8b') when $s_{i,j}$ is known. ($\eta_{i,j-1}$, of course, is known.) Eqs. (8b') for $s_{i,j} > g(\eta_{i,j})$ can be written as:

$$\dot{\eta}_{i,j} = F(s_{i,j}, \eta_{i,j-1} + \dot{\eta}_{i,j}\Delta t).$$

If this equation can be solved for $\dot{\eta}_{i,j}$ explicitly, then the calculation is straightforward. Otherwise, an iteration scheme may be devised for the calculation of $\dot{\eta}_{i,j}$ from $s_{i,j}$.

The inequalities expressed in Eqs. (12) are still valid for Eqs. (8a), (8b') and (8c), in view of the conditions Eqs. (2b) imposed on F. Therefore, there is no difficulty in the solution by successive approximations of this new system of equations. The existence and uniqueness of the solution follow automatically.

In [3], it was pointed out that the solution of the differential equation of motion with strain rate function represented by Eqs. (2) satisfies the minimum principle; the stress s cannot have a minimum value in the plastic region. To see that the finite difference equations, Eqs. (8a), (8b') and (8c), do possess the same minimum principle, one can eliminate $v_{i,j}$ from Eqs. (8a), (8b') and (8c) and obtain a system of equations similar to Eqs. (10b):

$$s_{i+1,j} - 2s_{i,j} + s_{i-1,j} = \frac{1}{r}\left[F(s_{i,j}, \eta_{i,j}) - F(s_{i,j-1}, \eta_{i,j-1})\right] \qquad (13a)$$

where $i = 1,2,.....,n-1$. The equations for $i = 0$ and n are not needed. Now, by the mean value theorem, the right-hand side of Eq. (13a) can be written as

$$F(s_{i,j}, \eta_{i,j}) - F(s_{i,j-1}, \eta_{i,j-1}) = (s_{i,j} - s_{i,j-1})\,\bar{F}_s + (\eta_{i,j} - \eta_{i,j-1})\,\bar{F}_\eta$$

$$= (s_{i,j} - s_{i,j-1})\,\bar{F}_s + \dot{\eta}_{i,j}\,\bar{F}_\eta\,\Delta t$$

$$= (s_{i,j} - s_{i,j-1})\,\bar{F}_s + F(s_{i,j}, \eta_{i,j})\,\bar{F}_\eta\,\Delta t$$

where $\bar{F}_s = F_s(\bar{s}_{i,j}, \bar{\eta}_{i,j})$, $\bar{F}_\eta = F_\eta(\bar{s}_{i,j}, \bar{\eta}_{i,j})$

$$\bar{s}_{i,j} = \theta s_{i,j} + (1 - \theta)s_{i,j-1}$$

$$\bar{\eta}_{i,j} = \theta \eta_{i,j} + (1 - \theta)\eta_{i,j-1} \qquad 0 < \theta < 1.$$

Therefore,

$$F(s_{i,j}, \eta_{i,j}) = \frac{1}{1-\bar{F}_\eta \Delta t}\left[F(s_{i,j-1}, \eta_{i,j-1}) + (s_{i,j} - s_{i,j-1})\,\bar{F}_s\right],$$

and Eq. (13a) becomes

$$s_{i+1,j} - 2s_{i,j} + s_{i-1,j} = \frac{1}{r(1-\bar{F}_\eta \Delta t)}\left[\Delta t \bar{F}_\eta F(s_{i,j-1}, \eta_{i,j-1}) + (s_{i,j} - s_{i,j-1})\bar{F}_s\right]. \qquad (13b)$$

Since $\bar{F}_s > 0$, $\bar{F}_\eta \leq 0$ by Eqs. (2b), Eq. (13b) satisfies the conditions of the minimum principle as shown in Lemma II of [5]. Thus $s_{i,j}$ cannot have its minimum at an interior point.

As an illustration, we take the strain rate function represented by Eqs. (3) with $\lambda = 1$. The results for $k = 1$, $v_o = 5$ and $p = 1$ to 5 are shown in Figs. 6 to 10. In all these calculations, the same mesh size ($\Delta x = 0.05$, $\Delta t = 0.025$) is used as for the previous example.

For p = 1, the problem is linear and the analytic solution can be obtained by using the Laplace transform. This is shown by the bold face lines in Fig. 7B for the solution before unloading occurs. It is seen that the differences between the exact and numerical solutions are indistinguishable for larger t.

To investigate the accuracy for p other than one, we consider the example for p = 3. When Δx is decreased, the solution does not seem to improve in any way. For smaller Δt, however, the solution does depend on Δt as shown in Fig. 5. Here we see that the unloading time t_o and the total strain $\eta(0, t_o)$ at the free end vary nearly linearly with Δt. For more detailed comparisons, the solution for p = 3 with $\Delta t = 0.0125$ (which is half the original interval $\Delta t = 0.025$) is shown in Figs. 6B and 7B by the dotted lines. The results are fairly good for $x \neq 0$. In general, the result is qualitatively satisfactory even for x = 0, if not quantitatively. The difficulty in the accuracy of the solution at x = 0 is the fact that the original differential equation has a singular initial condition while the approximate finite difference equation does not (and from the numerical point of view cannot) have this kind of singularity.

Figures 6-12 present curves showing plots of various quantities as functions of x or t. Figures 6-10 show results for impact conditions k = 1, $v_o = 5$; while Figs. 11 and 12 are for k = 1 and 10, with v_o ranging from 0.1 to 20.

The most interesting single feature of these results is perhaps the appearance of qualitative as well as quantitative contrasts between the cases $\lambda = 0$ and $\lambda = 1$, i.e. between a pure viscoplastic material (perfectly plastic behavior with yield stress dependent on strain rate), and a modified form of viscoplastic behavior in which strain hardening is considered. For example, considering final strains plotted as functions of x, Fig. 8A (for $\lambda = 0$) shows monotonically decreasing functions whereas in Fig. 8B (for $\lambda = 1$) the curves for $p \geq z$ show pronounced minima; that for p = 1 monotonically increases. The curves in Figs. 11 and 12 (for a variety of k and v_o magnitudes) also exhibit characteristic features

of being concave up for $\lambda = 0$ and concave down for $\lambda = 1$, at the point $x = 1$. This difference between the two media was proved analytically for $p = 1$ in [3], and the present calculations suggest that it holds also for the non-linear materials considered here.

The curves of Figs. 11 and 12 show final strains $\eta_f(x)$ in ratio to the strains η_f^* computed from an analysis which assumes that strains and stresses are at all times uniform along the specimen rod. This simplified analysis is outlined in the next section. It is seen that the final strains tend toward the result of the uniform strain theory as either k or v_o increases, but the effect of increasing k is particularly strong.

Further remarks on physical interpretation of these results are given in the final section.

4. Uniform Strain Analysis

As the striking mass or impact velocity is increased, the strains tend toward a uniform distribution along the rod. An approximate theory assuming uniform stress and strain is presented here, appropriate for sufficiently large k or v_o.

If $v(t)$ is the velocity of the striking mass, since all quantities are independent of x the equations of motion and strain rate behavior are

$$s(t) = - kv_t(t)$$

$$\eta_t(t) = F(s,\eta) = v(t)$$

Eliminating s and v between these equations,

$$\eta_t = F[-k\eta_{tt}, \eta] \qquad (14a)$$

with the initial conditions

$$\eta(0) = 0, \quad \eta_t(0) = v_o. \tag{14b}$$

Equations (14) can be reduced to a first order equation. Let

$$\eta_t = q.$$

Then
$$\eta_{tt} = \frac{dq}{d\eta} q$$

and Eqs. (14) become

$$q = F[-kq \frac{dq}{d\eta}, \eta] \tag{15a}$$

$$q = v_o \text{ when } \eta = 0. \tag{15b}$$

If Eq. (15a) can be solved for $dq/d\eta$, it is convenient to put it in the form:

$$\frac{d\eta}{dq} = f(q,\eta). \tag{16}$$

Conventional methods of integrating first order differential equations can be applied to Eq. (16) with initial condition (15b). For comparison with the results of previous sections, we take F as expressed by Eq. (3). Then Eq. (16) becomes

$$\frac{d\eta}{dq} = - \frac{kq}{1 + \lambda\eta + q^{1/p}} \tag{17a}$$

with the initial condition

$$q = v_o, \quad \eta = 0. \tag{17b}$$

Our object is to find the final strain η_f^* which is the value of η at $q = 0$. The integration of Eq. (17) was done by electronic computer, and the values of η_f^* have been used in presenting the results of the complete solution in Figs. 11 and 12.

Equation (17) can be solved analytically in a closed form when $\lambda = 0$ with p integer or $\lambda \neq 0$ with $p = 1$. For $\lambda = 0$ with p integral, the solution is given in [2]. For $\lambda \neq 0$ and $p = 1$, the solution is

$$\lambda\eta_f^* + 1 = (1 + v_o + 2\mu)^{1/2} \left(\frac{v_o + 2 - \sqrt{v_o^2 - 8\mu}}{v_o + 2 + \sqrt{v_o^2 - 8\mu}} \right)^{v_o/2\sqrt{v_o^2 - 8\mu}} \quad \text{if } v_o^2 > 8\mu$$

$$\lambda\eta_f^* + 1 = (1 + \sqrt{2\mu}) \exp \frac{-\sqrt{2\mu}}{1 + \sqrt{2\mu}} \quad \text{if } v_o^2 = 8\mu \qquad (18)$$

$$\lambda\eta_f^* + 1 = (1 + v_o + 2\mu)^{1/2} \exp \left[- \frac{v_o}{\sqrt{8\mu - v_o^2}} \tan^{-1} \frac{\sqrt{8\mu - v_o^2}}{2 + v_o} \right] \quad \text{if } v_o^2 < 8\mu$$

where $\mu = \frac{\lambda}{2} k v_o^2$.

5. Discussion

In the preceding work the non-dimensional variables listed in Table 1 were used for convenience in the computations. For physical interpretations, these have disadvantages of mixing physical quantities specifying the impact conditions with those describing the material behavior. Also the quantities specifying plastic and viscous properties are intermingled. For example, the impact data are specified by the quantities $k = G/\rho AL$ and $v_o = V_o/DL$, and the parameter $\lambda = E_1 \rho D^2 L^2/\sigma_o^2$ is used to specify the strain hardening behavior. These are convenient for numerical work,

but make it difficult to draw comparisons between different materials and impact conditions. The following dimensionless parameters have more obvious physical meaning and are more convenient for physical interpretations:

Table 2

Independent variables: $x = \frac{X}{L}$, $\tau = \frac{\sqrt{\sigma_o/\rho}}{L} T$

Impact parameters: $k = \frac{G}{AL}$, $\phi_o = \frac{v_o}{\sqrt{\sigma_o/\rho}}$

$$\varepsilon_f^o = \frac{1}{2} k \phi_o^2 = \frac{G V_o^2}{2\sigma_o AL}; \quad \tau_f^o = k\phi_o = \frac{G V_o}{\sigma_o A} \frac{\sqrt{\sigma_o/\rho}}{L}$$

Plasticity (strain hardening): $\beta = \frac{E_1}{\sigma_o}$

Strain rate dependence: $\nu = \frac{\sqrt{\sigma_o/\rho}}{DL}$, p

Note relations with previously defined v_o, λ, η, t:

$$\nu\phi_o = v_o \qquad \varepsilon_f^o = \frac{1}{2} k \frac{v_o^2}{\nu^2}$$

$$\beta = \lambda\nu^2 \qquad \tau_f^o = k \frac{v_o}{\nu}$$

$$\nu^2\varepsilon = \eta \qquad \tau = \frac{t}{\nu}$$

In the new parameters of Table 2, the quantity $\sqrt{\sigma_o/\rho}$, with dimensions of velocity, is a convenient reference characteristic of the material. There are two independent parameters specifying the impact data, which can be defined in various ways but in any case enable one to specify the initial energy and initial momentum of the striking mass. The most useful impact parameter is ε_f^o, which

represents the final strain in the specimen under the idealized conditions of uniform strain and stress, all the energy being imagined as absorbed at the yield stress σ_o with neither strain hardening nor rate sensitivity. Since ε_f^o is also the initial kinetic energy of the striking mass, in a non-dimensional form, the energy ratio R of initial energy to the maximum elastic strain energy can be written as

$$R = \frac{GV_o^2}{2} \div \frac{\sigma_o^2}{2E} AL = \frac{2E}{\sigma_o} \varepsilon_f^o \tag{19}$$

A necessary condition for validity of a rigid-plastic treatment is that $R >> 1$; for the impact problem this would be also a sufficient condition. For ε_f^o of the order of 0.05 or more, R would be roughly 100 or larger for one of the structural metals, and presumably a rigid-plastic treatment would apply with good accuracy.

Similarly, the parameter τ_f^o is the (non-dimensional) duration time of the deformation; it is also the initial momentum in a non-dimensional form.

Estimates of the approximate ranges of numerical values of $\sqrt{\sigma_o/\rho}$ and other parameters representing material properties were given in [2] as follows:

	σ_o(ksi)	$\sqrt{\sigma_o/\rho}$ (in-sec^{-1})	$E\rho/\sigma_o = \beta$	p	$\frac{\sqrt{\sigma_o/\rho}}{D} = \nu L$ (in.)
Mild steel	30	6,500	6-9	4-6	25-200
Aluminum alloy 6061-T6	40	12,500	1-4	4-8	0.05-2

With these ranges in mind, the physical significance of the illustrative cases treated in this report can be seen. Results have been given for k = 1, 10; v_o = 1, 5, 20; λ = 0, 1. Effects of changes of <u>one</u> of the impact variables k or

ε_f^o (or ϕ_o), or of the material parameters ν or β, can be observed if all the remaining quantities are held constant. For example, suppose ν and β have constant values; changes of k or of v_o then show the effects of changing impact conditions on specimens of a given material. Table 3 shows the numerical values of ϕ_o, ε_f^o, and β assuming $\nu = 20$, which correspond to the magnitudes of k, v_o, and λ used in the calculations of this report.

Table 3

Interpretation of impact data with $\nu = 20$

$\varepsilon = n/\nu^2 = n/400$

$\beta = 0$ for $\lambda = 0$

$\beta = 400$ for $\lambda = 1$

v_o	ϕ_o	ε_f^o	
		k = 1	k = 10
0.1	0.005	$.125 \times 10^{-4}$	1.25×10^{-4}
1	0.05	$.125 \times 10^{-2}$	.0125
5	0.25	.0313	0.313
20	1.0	.5	5

The results shown in Figs. 11 and 12 thus correspond to tests on a material of moderately strong rate sensitivity and either no strain hardening or very large strain hardening. The range of impact energies considered is too wide to be realistic; at the small values of v_o the condition R >> 1 for a rigid-plastic treatment could hardly be satisfied, while at the largest values of v_o and k the strains are unrealistically large.

Alternatively one can take the impact conditions constant and consider the effects of changing material parameters. However the relation $\beta = \lambda v^2$ shows that if λ is constant, a change in β accompanies one in v. The present calculations are therefore not suitable for comparing the responses of different materials under constant impact conditions. Further calculation for this purpose has been carried out, and will be presented in a companion report [6].

References

1. "Longitudinal Impact on Viscoplastic Rods -- Linear Stress-Strain Rate Law," T. C. T. Ting and P. S. Symonds, J. Appl. Mech., Vol. 31 (No. 2), pp. 199-207, June 1964.

2. "Longitudinal Impact on Viscoplastic Rods -- Approximate Methods and Comparisons," P. S. Symonds and T. C. T. Ting, J. Appl. Mech., 31, p. 611, December 1964.

3. "Longitudinal Impact on Viscoplastic Rods -- General Properties of Solutions," T. C. T. Ting, Tech. Rept. NSF-GP1115/4, Division of Engineering, Brown University, January 1964.

4. "A Strong Maximum Principle for Parabolic Equations," L. Nirenberg, Comm. Pure Appl. Math., 6, pp. 167-177, 1953.

5. "The Maximum-Minimum Principles for a Quasi-Linear Parabolic Finite Difference Equation," T. C. T. Ting, Quart. Appl. Math., 22, pp. 47-56, 1964.

6. "Impact on Rods of Non-Linear Viscoplastic Material -- Analysis and Experiments," P. S. Symonds. (In preparation.)

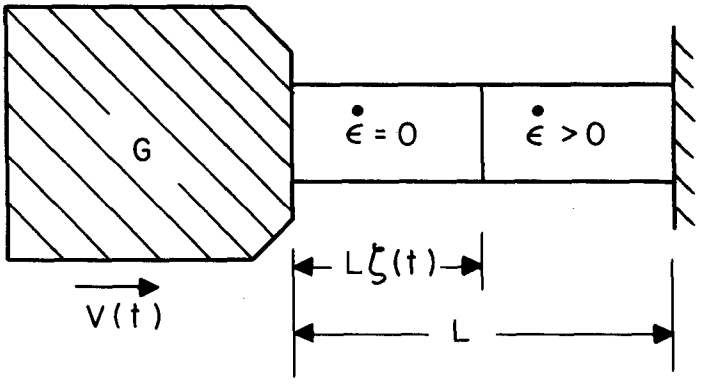

FIGURE 1

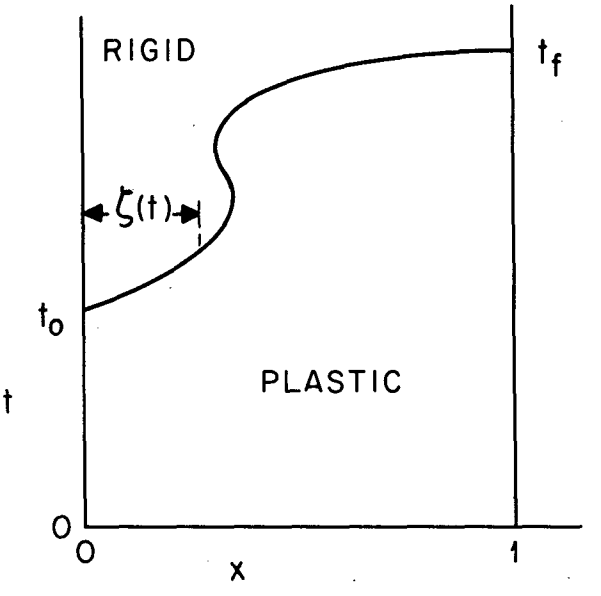

FIGURE 2

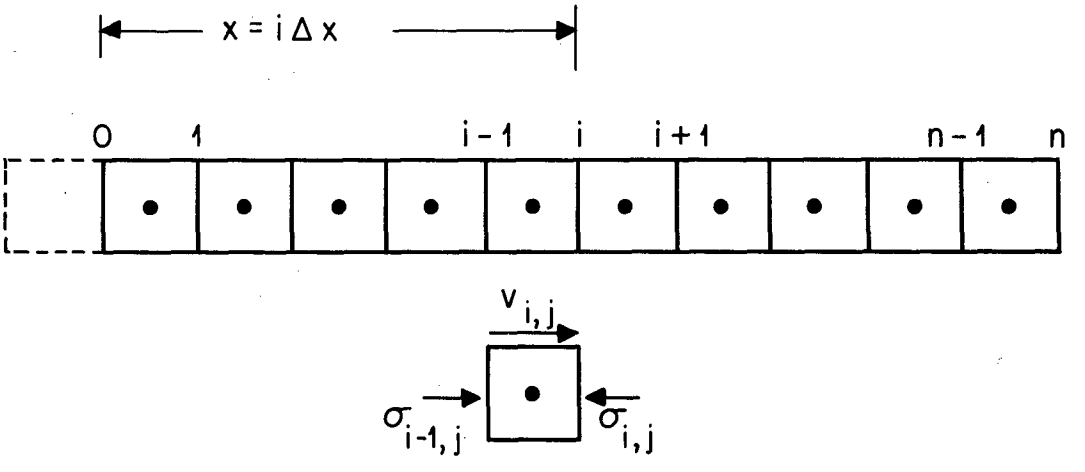

FIGURE 3

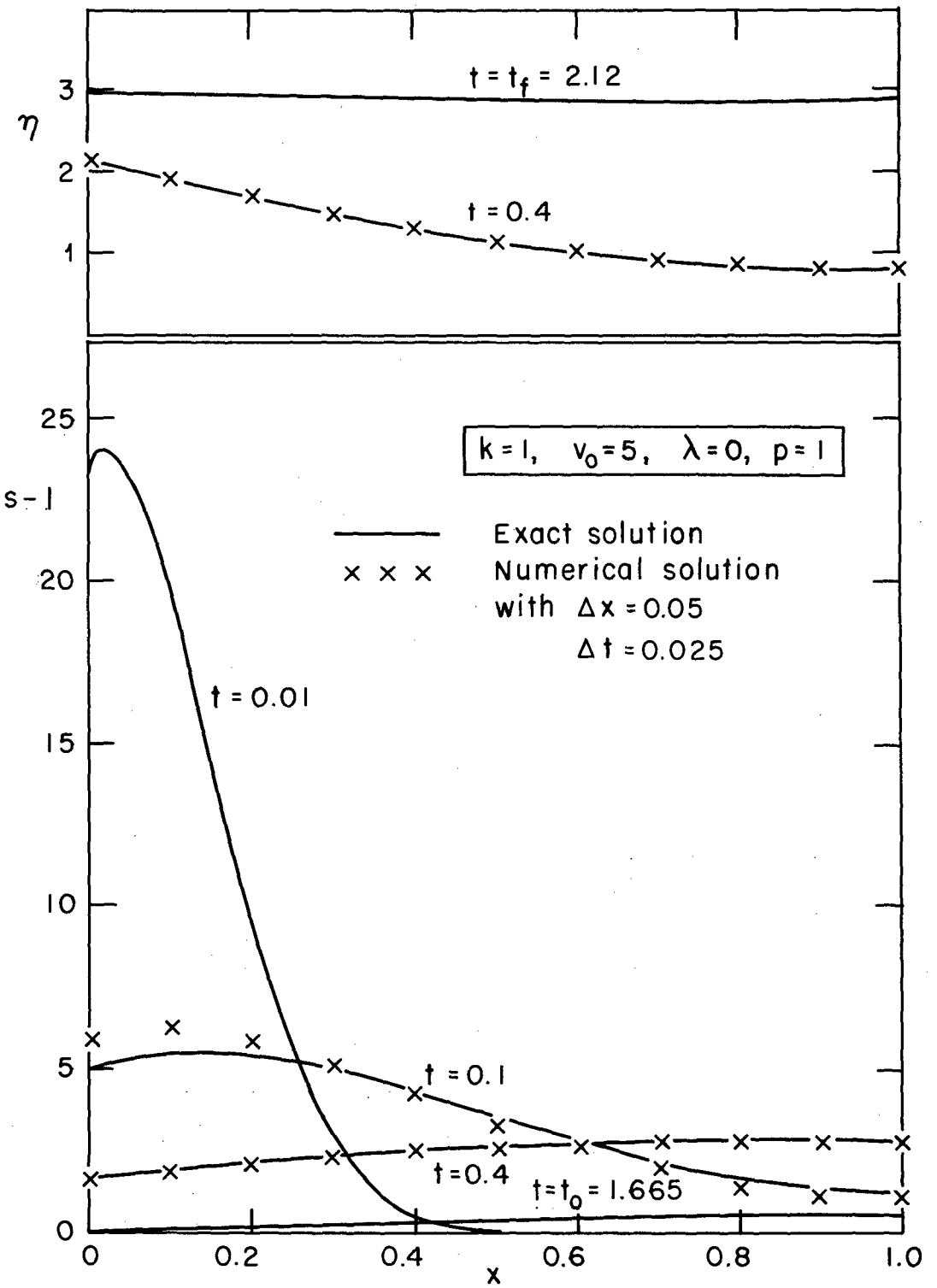
t = t_f = 2.12
η
3
2
1
t = 0.4
25
20
15
10
5
0
s - 1
k = 1, v_0 = 5, λ = 0, p = 1
Exact solution
Numerical solution
with Δx = 0.05
Δt = 0.025
t = 0.01
t = 0.1
t = 0.4
t = t_0 = 1.665
0
0.2
0.4
0.6
0.8
1.0
x

FIGURE 4

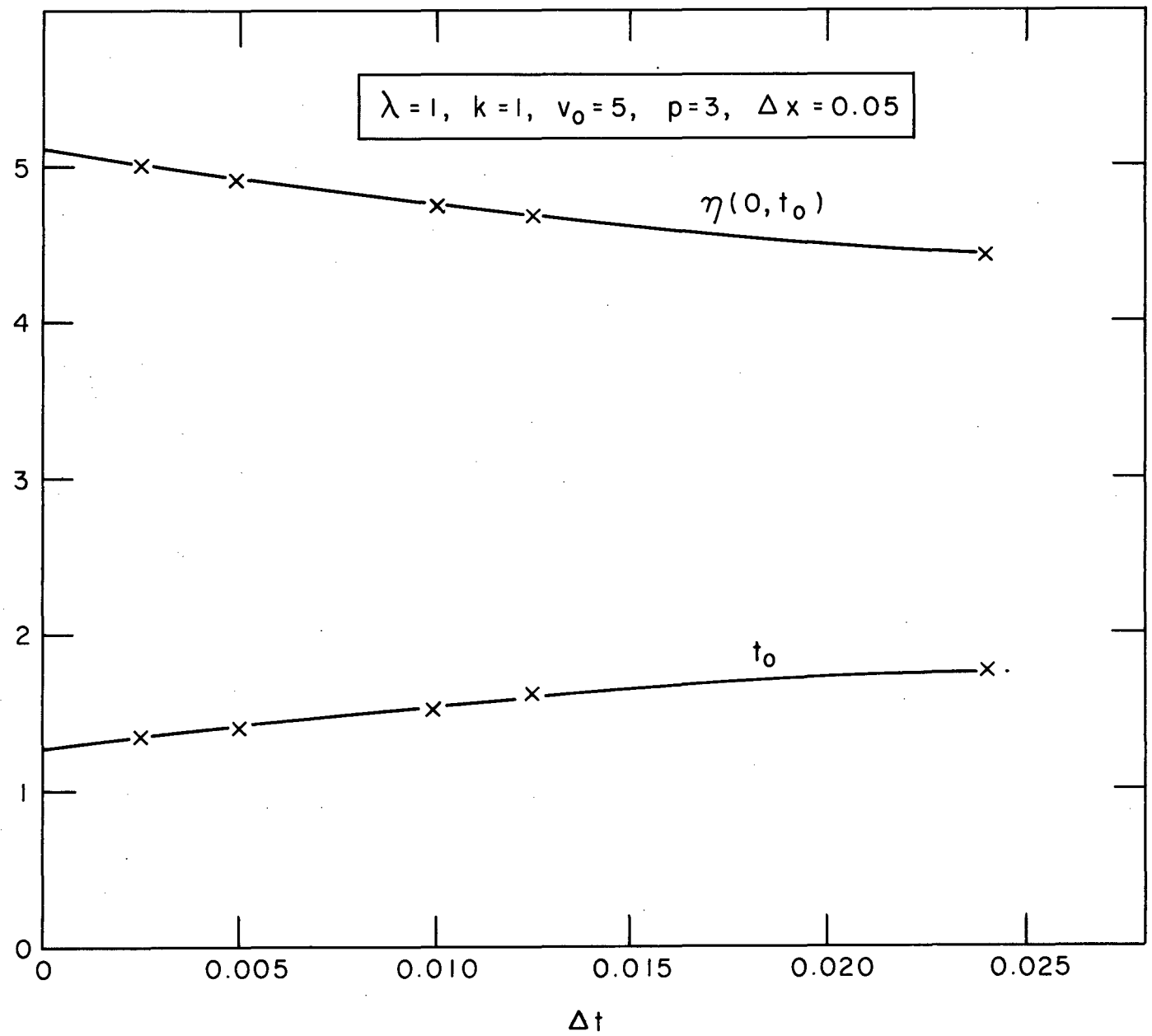

FIGURE 5

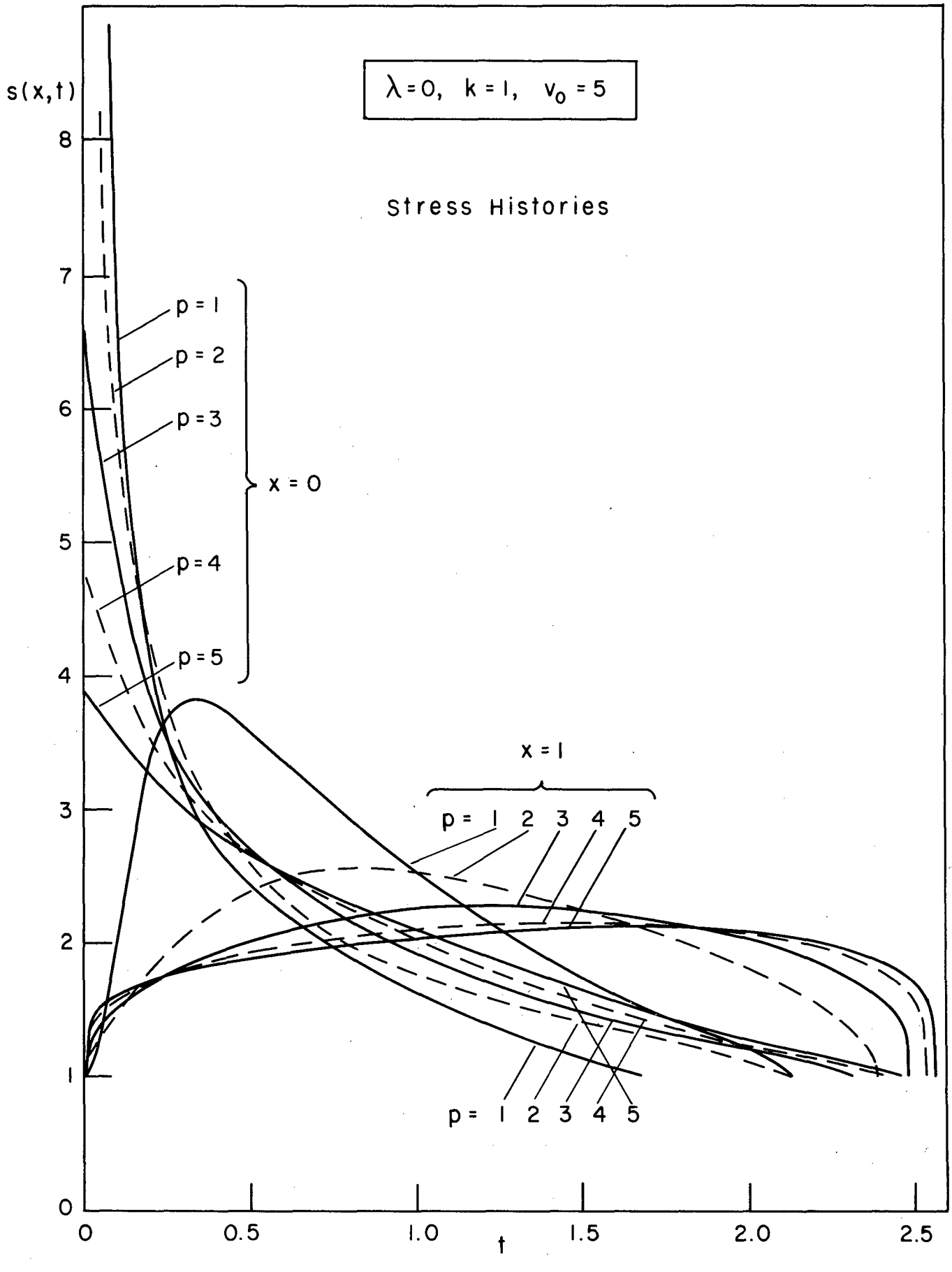
λ = 0, k = 1, v_0 = 5
Stress Histories
s(x,t)
8
7
6
5
4
3
2
1
0
p = 1
p = 2
p = 3
p = 4
p = 5
x = 0
x = 1
p = 1 2 3 4 5
p = 1 2 3 4 5
0
0.5
1.0
1.5
2.0
2.5
t

FIGURE 6A

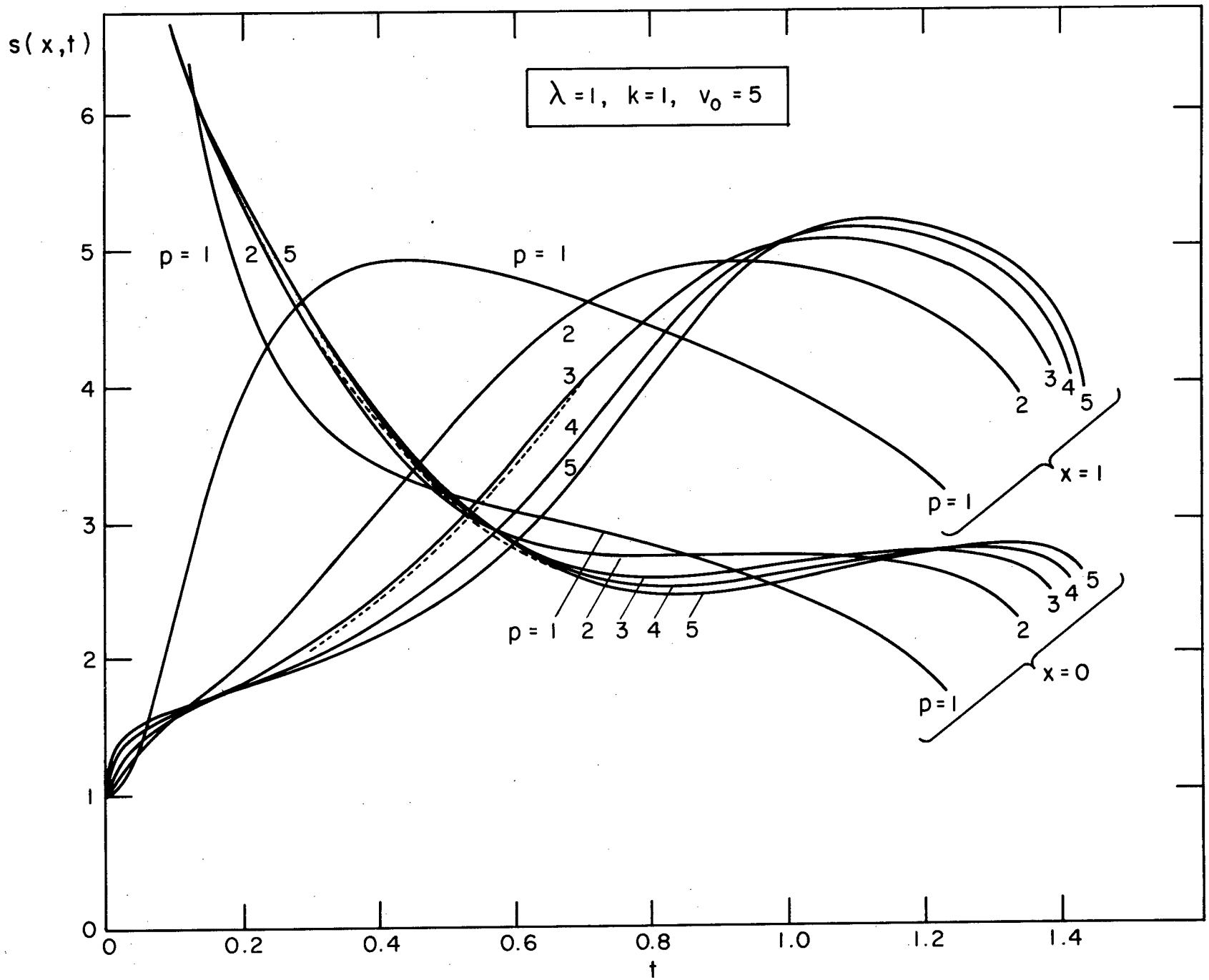
s(x,t)
λ = 1, k = 1, v0 = 5
p = 1 2 5
p = 1
2
3
4
5
2 3 4 5
p = 1
x = 1
p = 1 2 3 4 5
2 3 4 5
p = 1
x = 0
0
1
2
3
4
5
6
0
0.2
0.4
0.6
0.8
1.0
1.2
1.4
t

FIGURE 6B

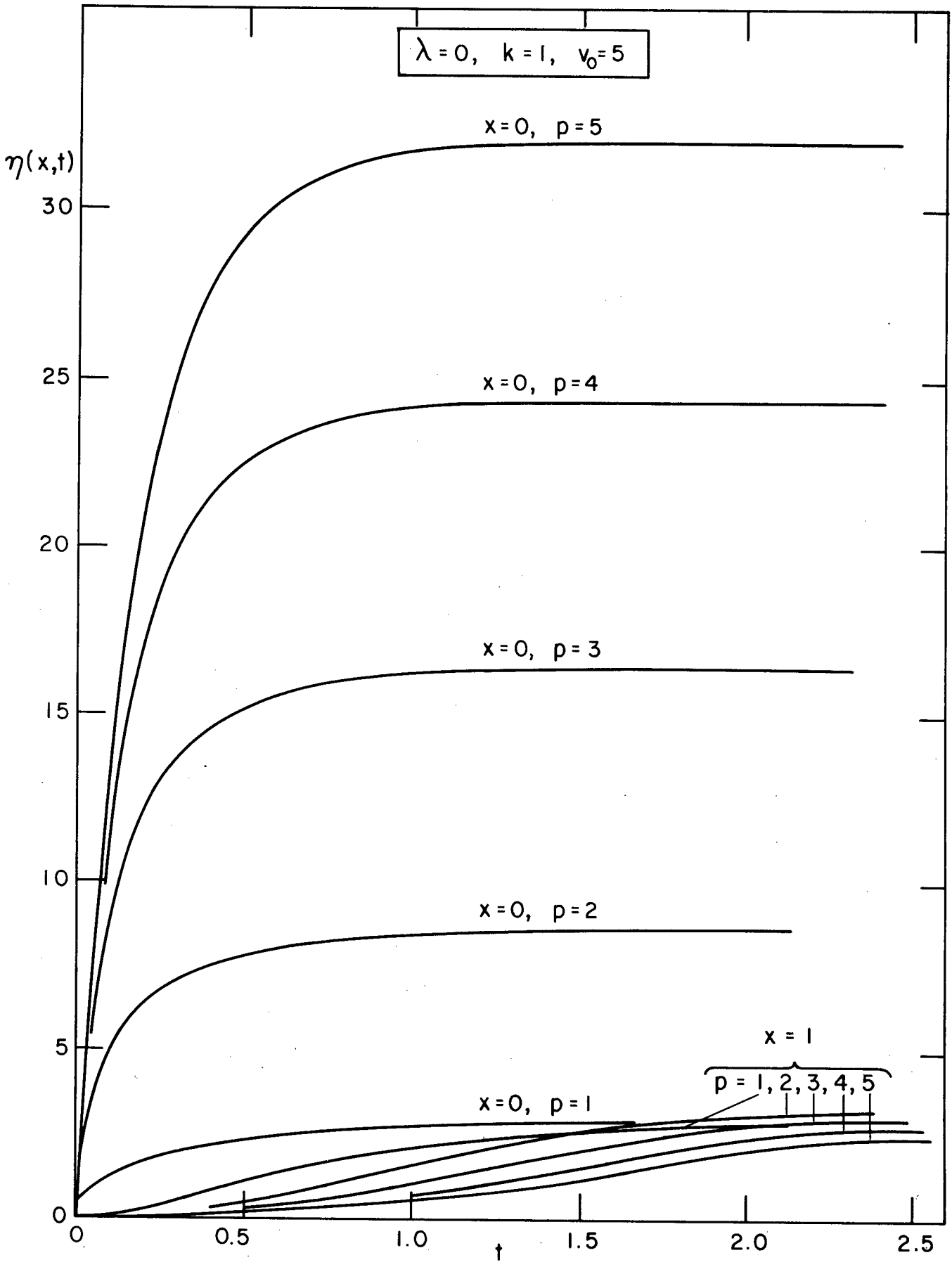
λ = 0, k = 1, v_0 = 5
η(x,t)
x = 0, p = 5
x = 0, p = 4
x = 0, p = 3
x = 0, p = 2
x = 0, p = 1
x = 1
p = 1, 2, 3, 4, 5
30
25
20
15
10
5
0
0
0.5
1.0
1.5
2.0
2.5
t

FIGURE 7A

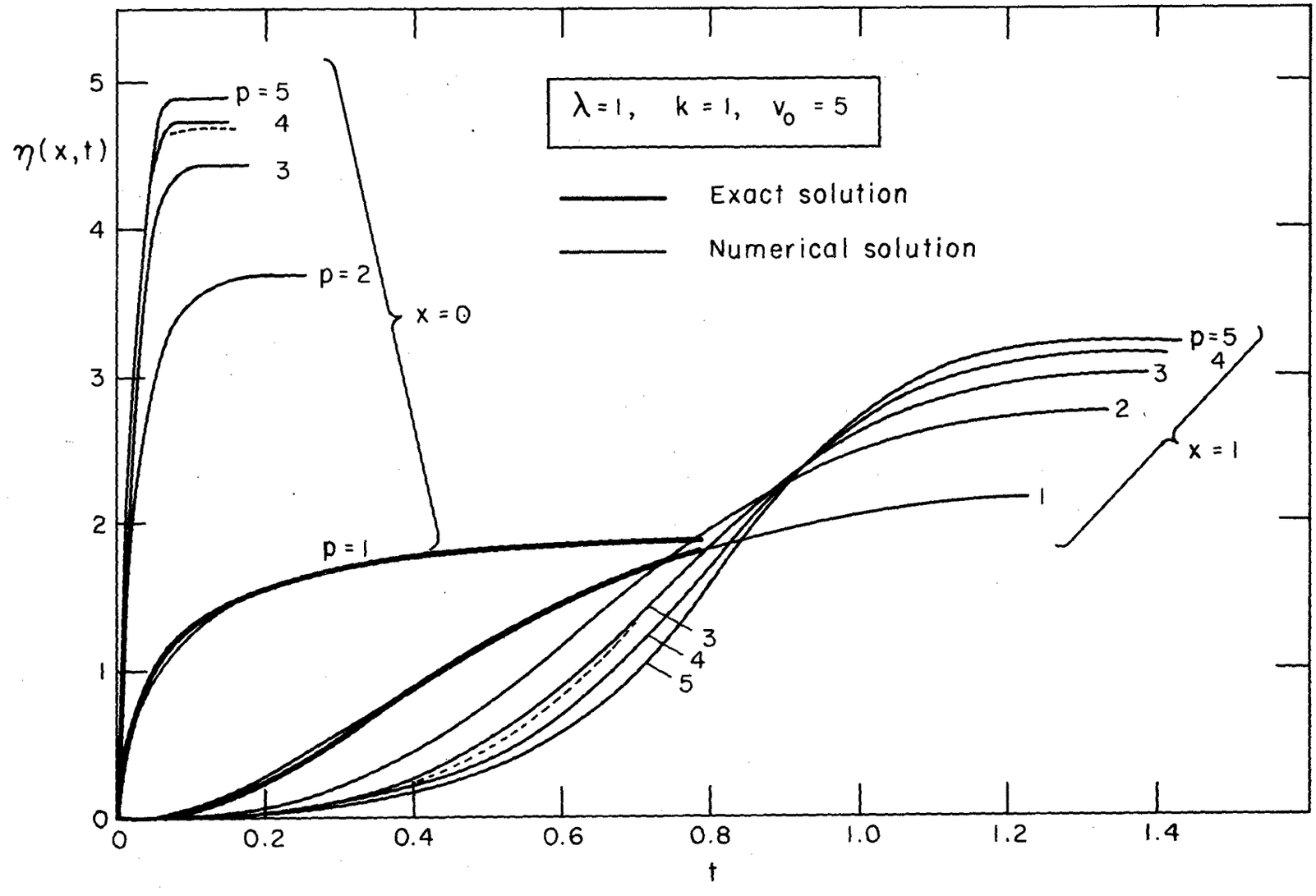
λ=1, k=1, v_0=5
Exact solution
Numerical solution
η(x,t)
t
x=0
x=1
p=5
4
3
2
1
p=2
p=1
0
0.2
0.4
0.6
0.8
1.0
1.2
1.4
5

FIGURE 7B

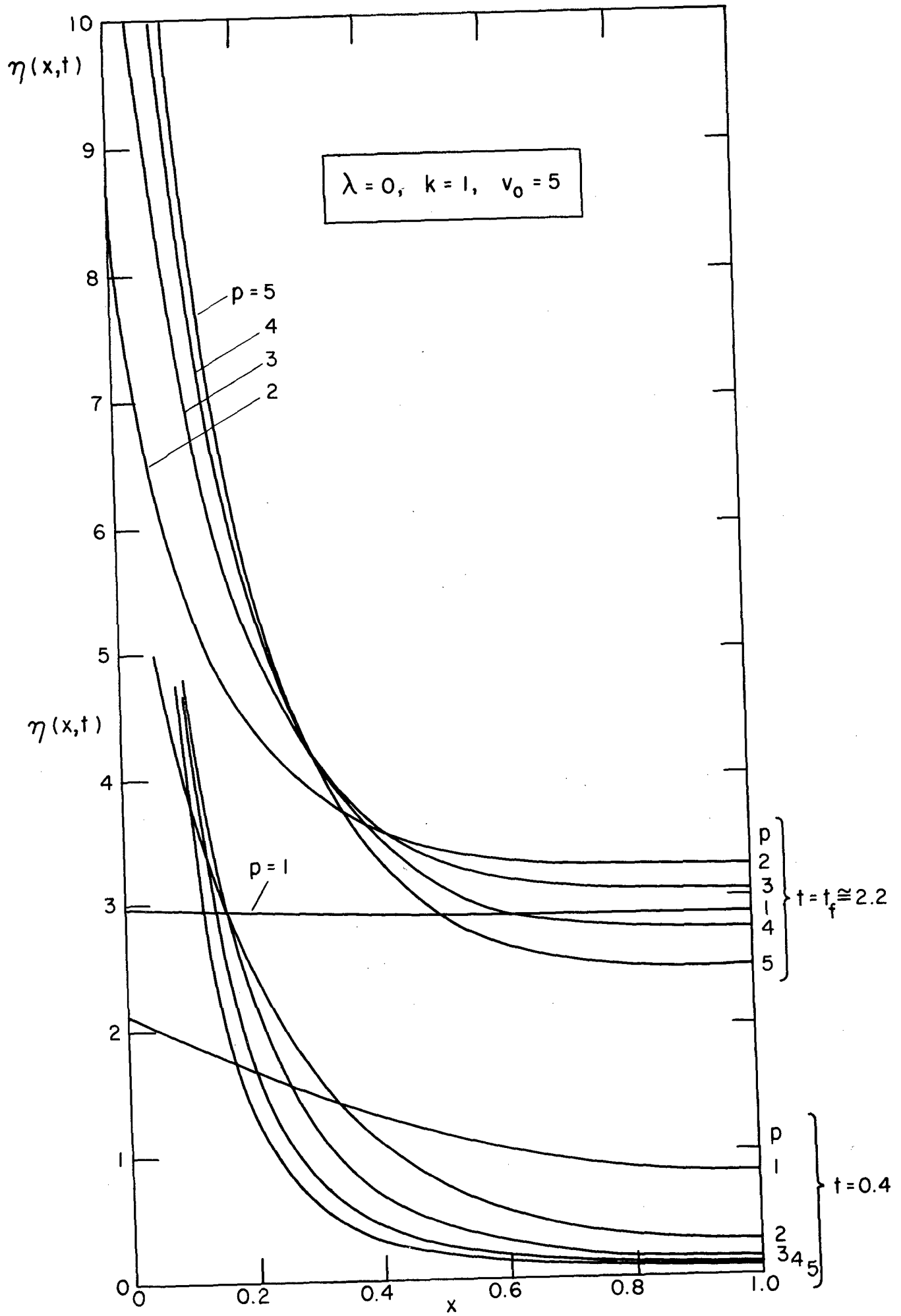
η(x,t)
10
9
8
7
6
5
4
3
2
1
0
λ = 0, k = 1, v0 = 5
p = 5
4
3
2
p = 1
η(x,t)
p
2
3
1
4
5
t = tf ≅ 2.2
p
1
2
3
4
5
t = 0.4
0
0.2
0.4
0.6
0.8
1.0
x

FIGURE 8A

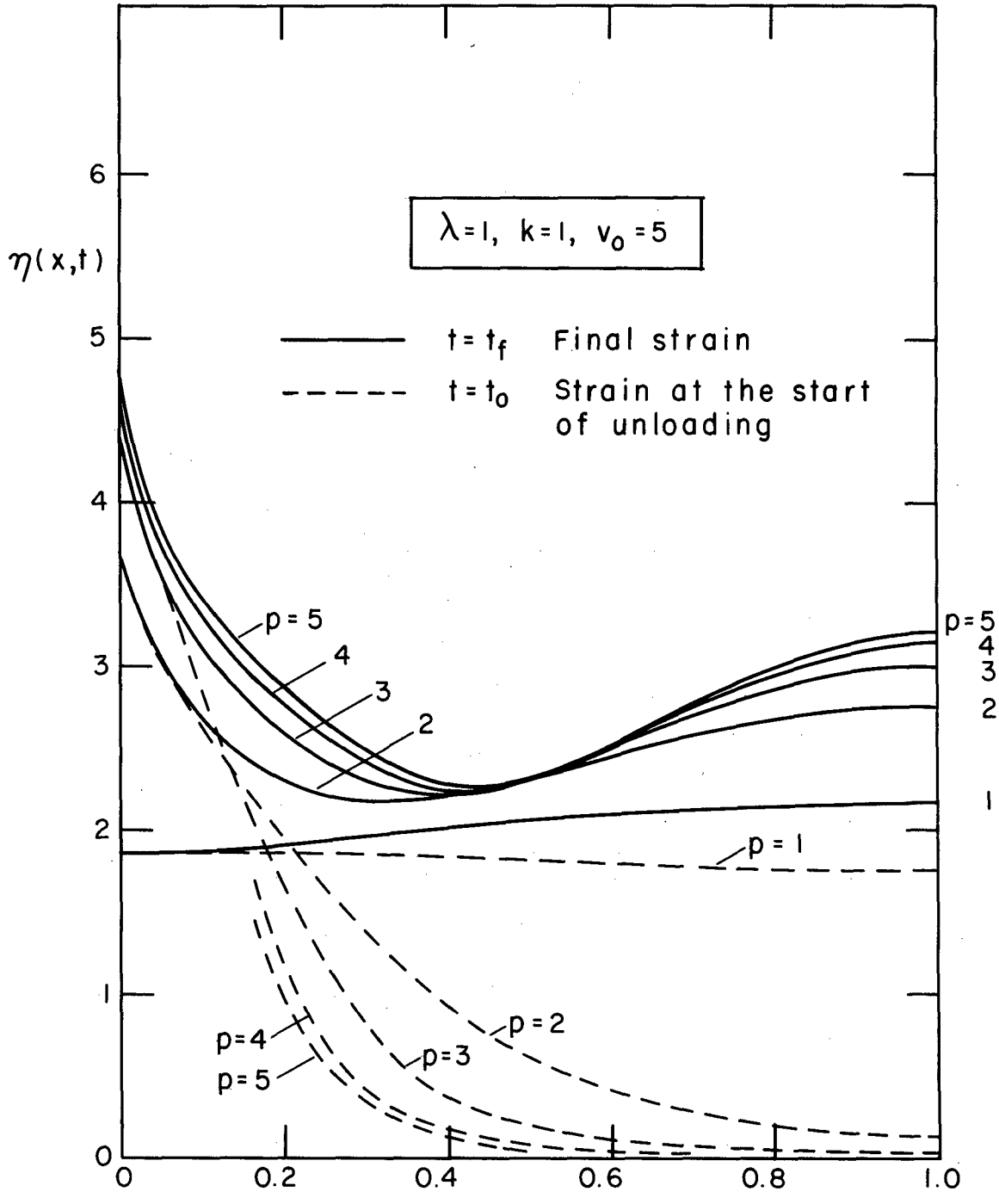
$\eta(x,t)$
$\lambda=1,\ k=1,\ v_0=5$
$t=t_f$ Final strain
$t=t_0$ Strain at the start of unloading
p = 5
4
3
2
1
p=4
p=5
p=3
p=2
p=1
0
1
2
3
4
5
6
0
0.2
0.4
0.6
0.8
1.0

FIGURE 8B

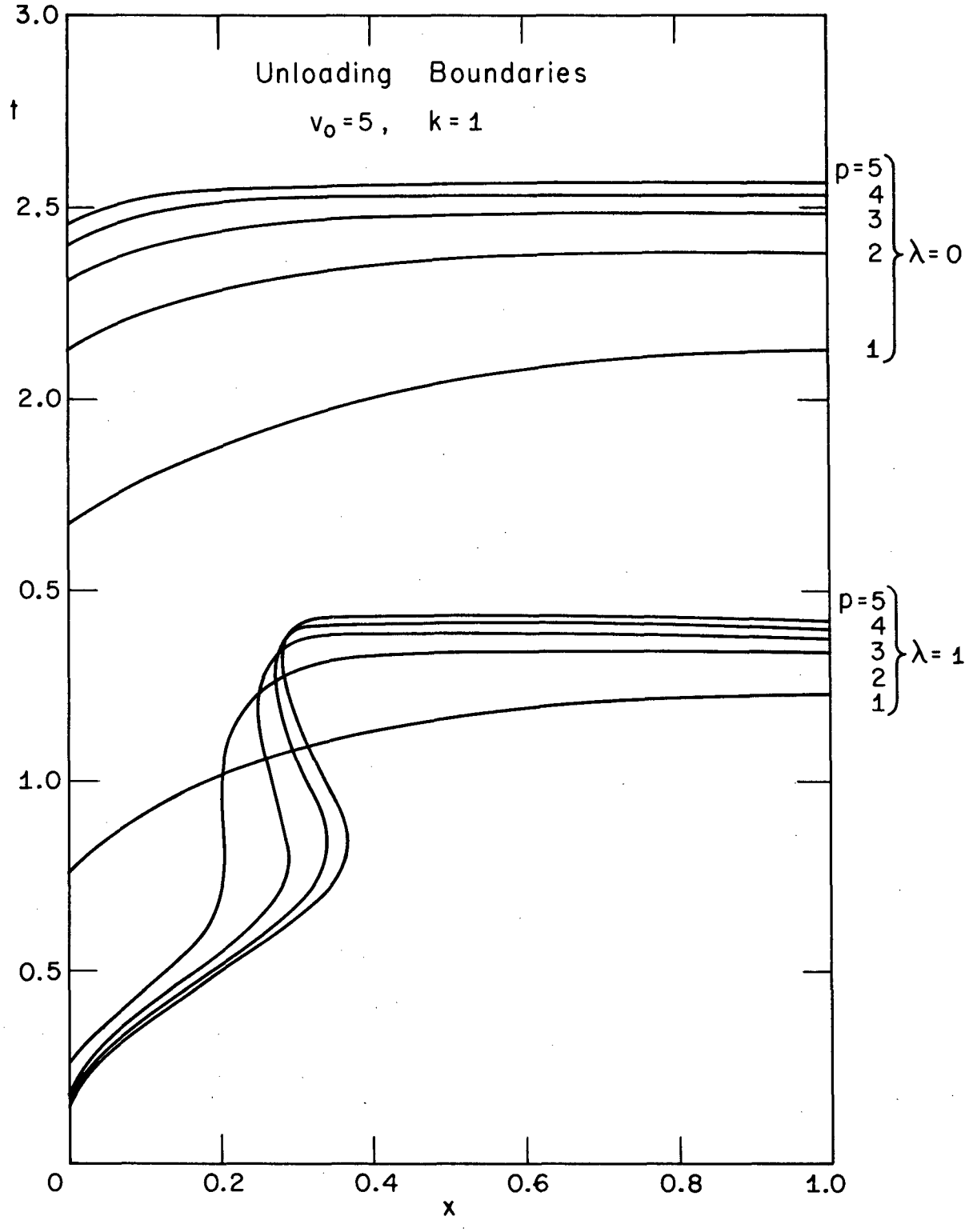
Unloading Boundaries
$v_0 = 5$, $k = 1$
t
x
3.0
2.5
2.0
0.5
1.0
0.5
0
0.2
0.4
0.6
0.8
1.0
p=5
4
3
2
1
λ=0
p=5
4
3
2
1
λ=1

FIGURE 9

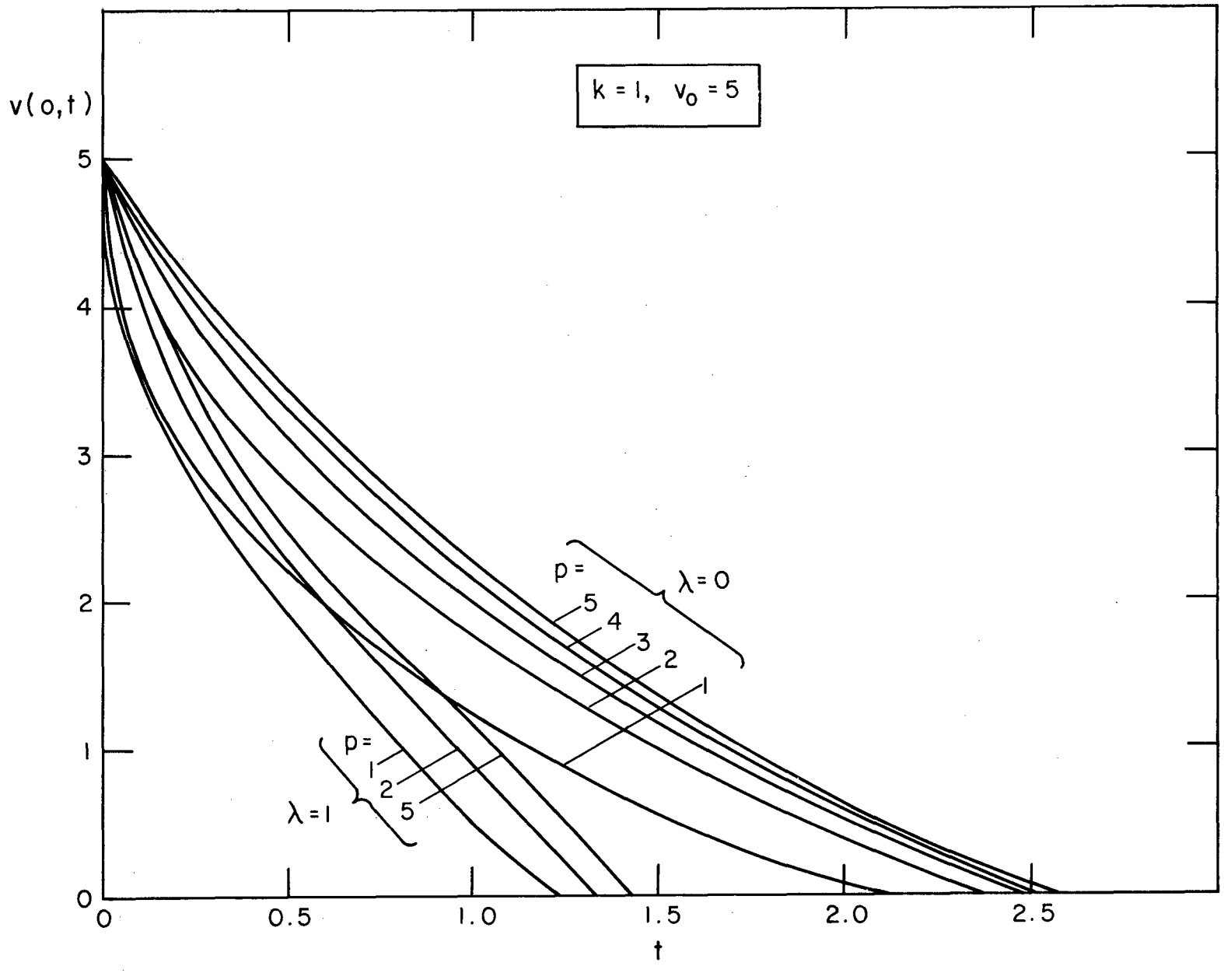

FIGURE 10

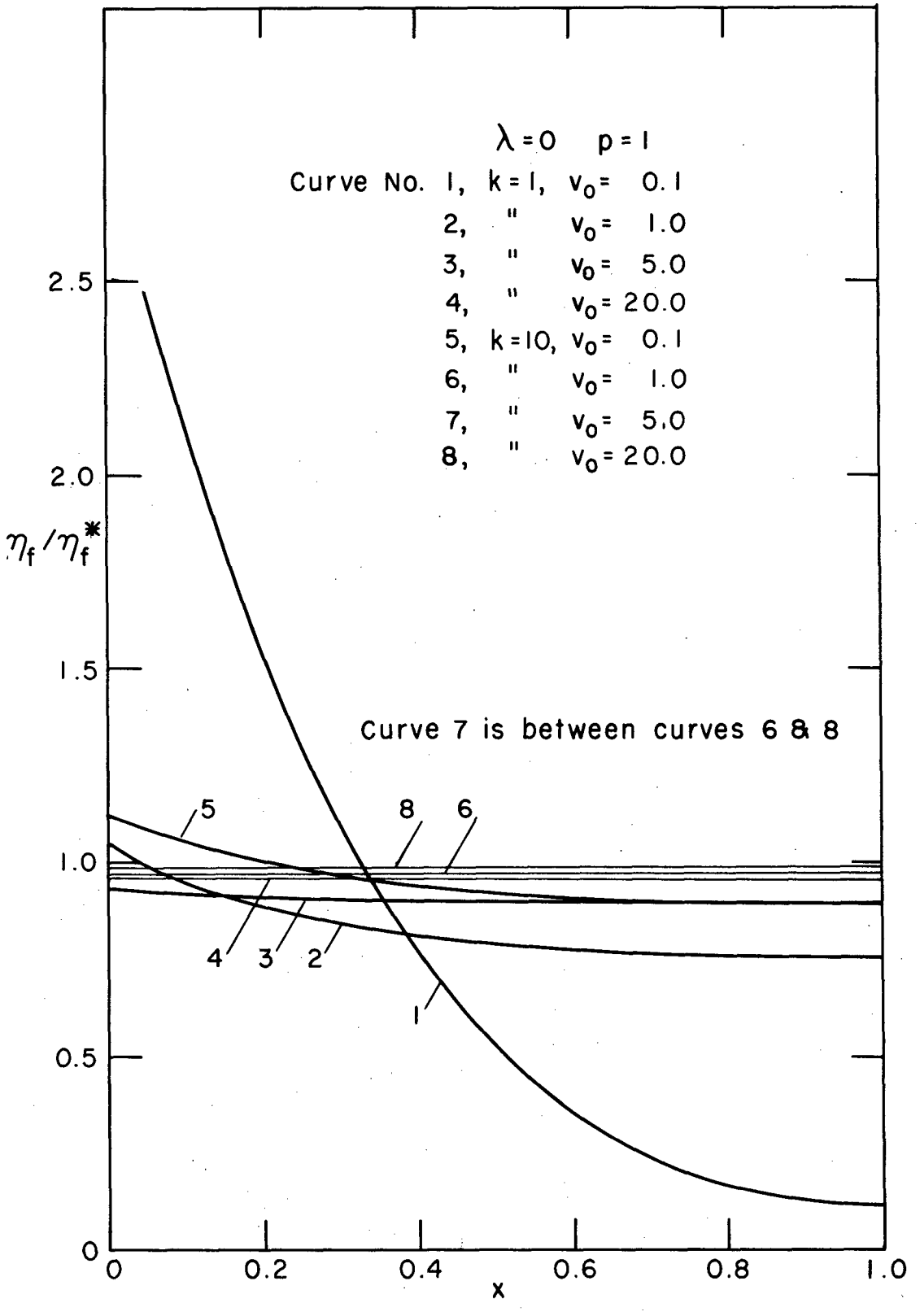
λ = 0 p = 1
Curve No. 1, k = 1, v_0 = 0.1
2, " v_0 = 1.0
3, " v_0 = 5.0
4, " v_0 = 20.0
5, k = 10, v_0 = 0.1
6, " v_0 = 1.0
7, " v_0 = 5.0
8, " v_0 = 20.0
Curve 7 is between curves 6 & 8
η_f / η_f^*
2.5
2.0
1.5
1.0
0.5
0
0
0.2
0.4
0.6
0.8
1.0
x
1
2
3
4
5
6
8

FIGURE IIA

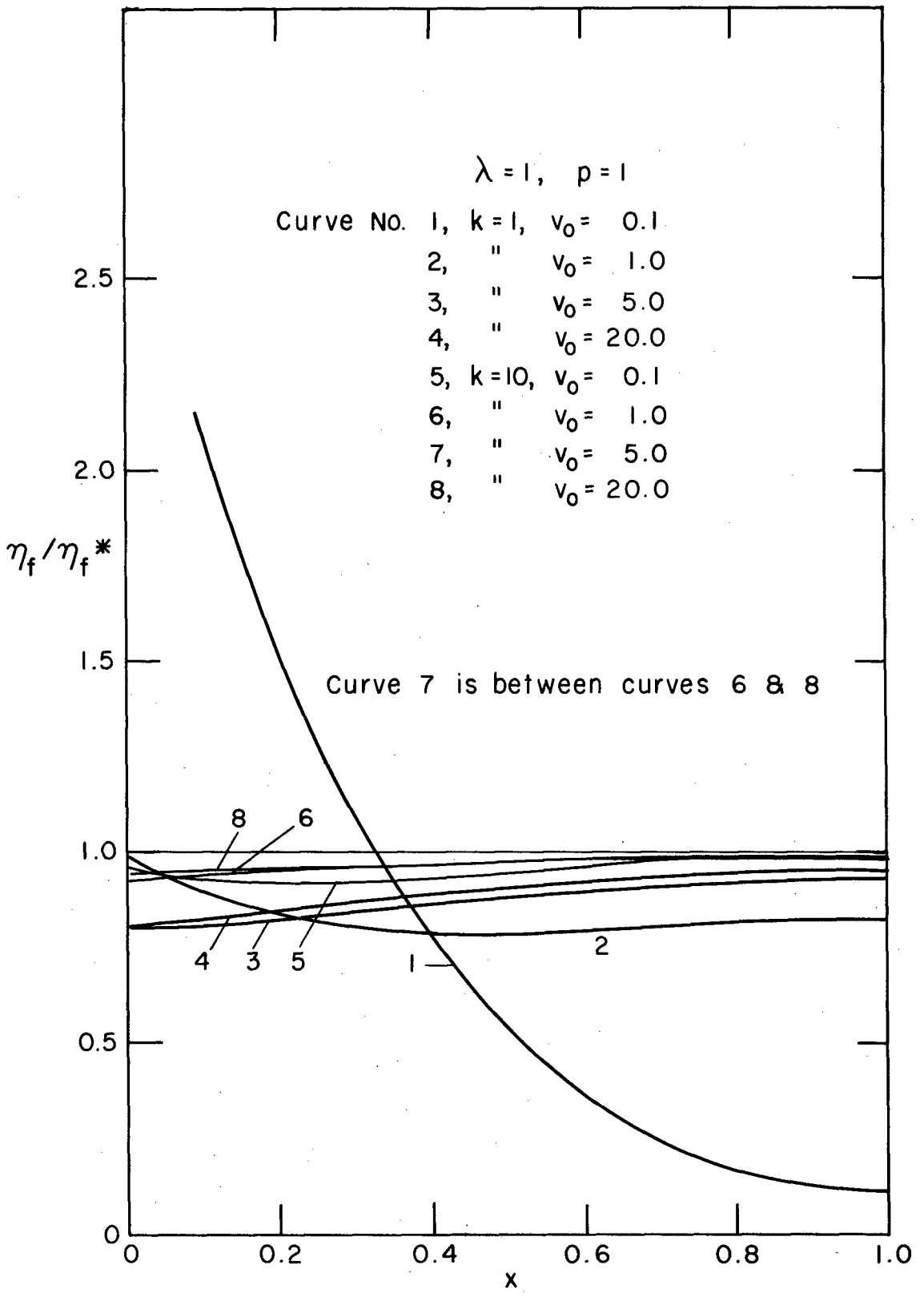
λ = 1, p = 1
Curve No. 1, k = 1, v_0 = 0.1
2, " v_0 = 1.0
3, " v_0 = 5.0
4, " v_0 = 20.0
5, k = 10, v_0 = 0.1
6, " v_0 = 1.0
7, " v_0 = 5.0
8, " v_0 = 20.0
Curve 7 is between curves 6 & 8
η_f / η_f^*
2.5
2.0
1.5
1.0
0.5
0
0
0.2
0.4
0.6
0.8
1.0
x
1
2
3
4
5
6
8

FIGURE 11B

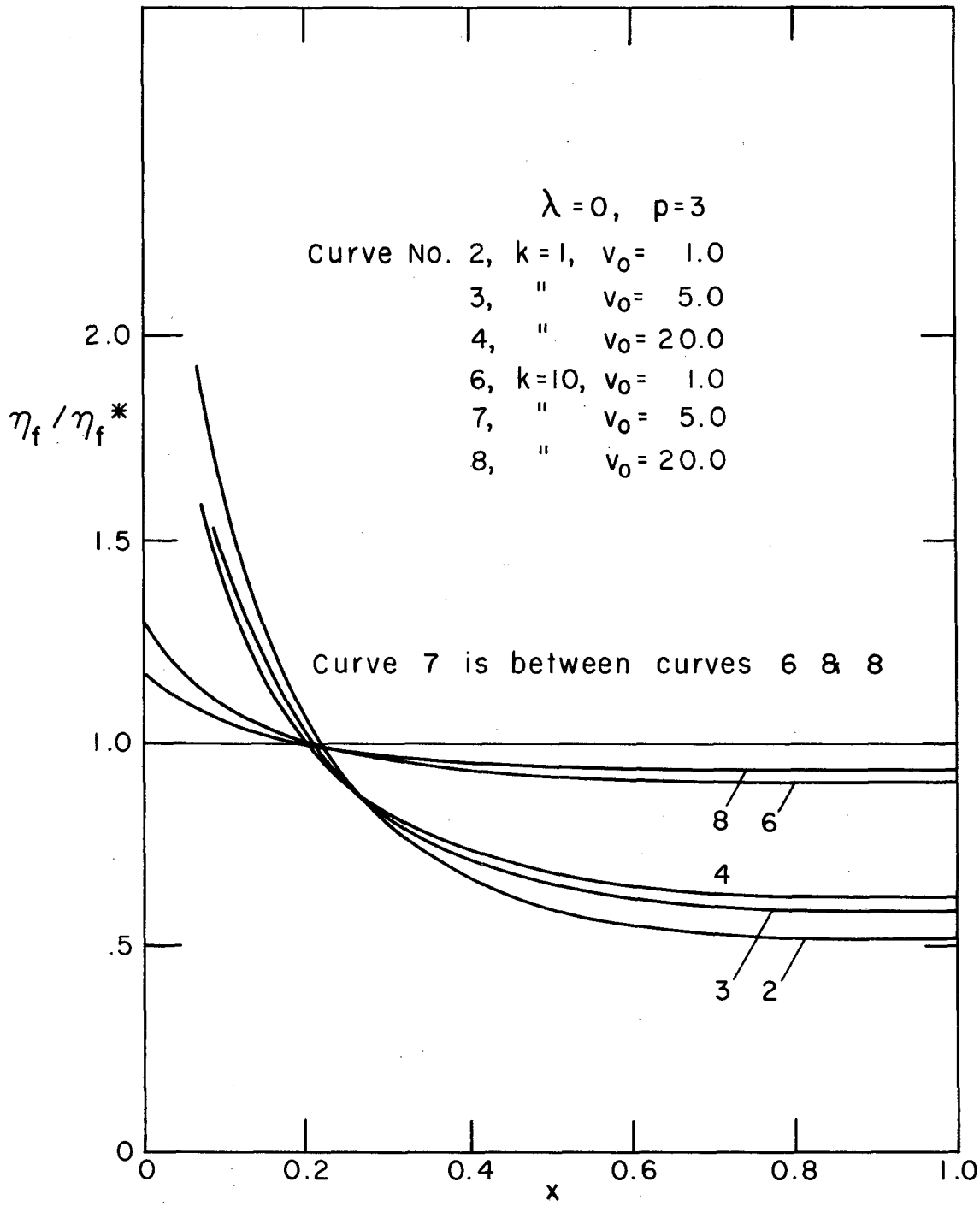
λ = 0, p = 3
Curve No. 2, k = 1, v0 = 1.0
3, " v0 = 5.0
4, " v0 = 20.0
6, k = 10, v0 = 1.0
7, " v0 = 5.0
8, " v0 = 20.0
Curve 7 is between curves 6 & 8
ηf / ηf*
2.0
1.5
1.0
.5
0
0
0.2
0.4
0.6
0.8
1.0
x
8
6
4
3
2

FIGURE 12A

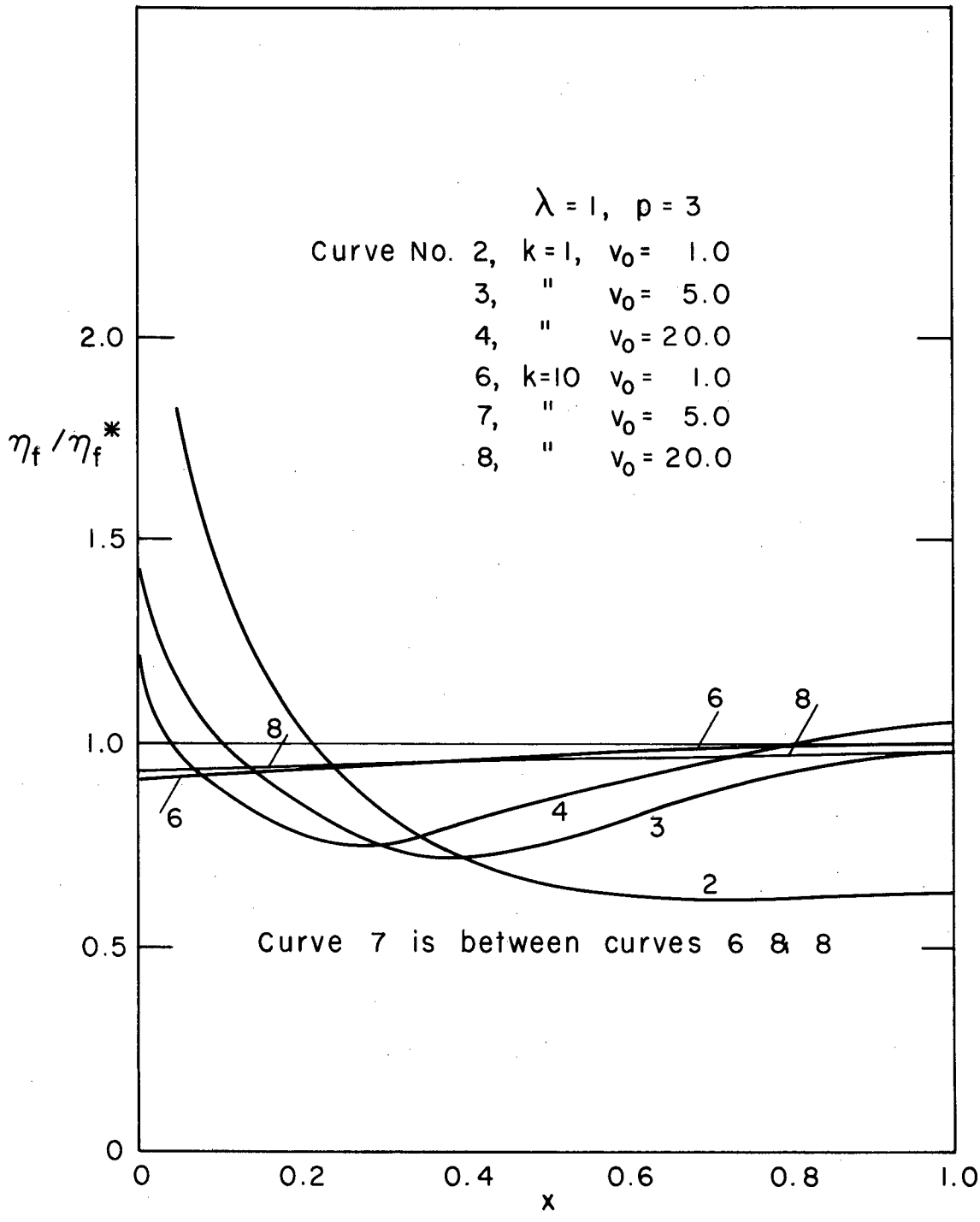
λ = 1, p = 3
Curve No. 2, k = 1, v_0 = 1.0
3, " v_0 = 5.0
4, " v_0 = 20.0
6, k=10 v_0 = 1.0
7, " v_0 = 5.0
8, " v_0 = 20.0
η_f / η_f^*
2.0
1.5
1.0
0.5
0
0
0.2
0.4
0.6
0.8
1.0
x
6
8
8
6
4
3
2
Curve 7 is between curves 6 & 8

FIGURE 12B